J. Fluid Mech. (1970), *vol.* 42, *part* 2, *pp.* 225–244
Printed in Great Britain

Instability of erodible beds

By FRANK ENGELUND
Hydraulic Laboratory, Technical University of Denmark

(Received 28 April 1969 and in revised form 14 November 1969)

The stability of a sand bed in an alluvial channel is investigated by a two-dimensional mathematical model, based on the vorticity transport equation. The model takes account of the internal friction and describes the non-uniform distribution of the suspended sediment. It turns out that the inclusion of the friction and of a definite model of the sediment transport mechanism leads to results rather different from those obtained previously by potential-flow analysis.

1. Introduction

The formation of varied sandwave patterns in erodible channels has attracted considerable attention in recent years, probably because it constitutes an interesting phenomenon in itself, and because of its significance to hydraulic engineering. For a thorough review, readers are referred to a recent monograph by Allen (1968).

The mechanics of dunes and antidunes was treated by Kennedy (1963) by means of a mathematical model considering the flow of a homogeneous ideal fluid over an erodible, sinusoidal bed. It was pointed out that a realistic picture required the assumption of a spatial lag between the maximum bed velocity and the maximum sediment transport rate.

Kennedy's theory was later supplemented with an analysis by Reynolds (1965).

Engelund & Hansen (1966) tried to develop a stability theory based on the flow of a real fluid over a sinusoidal movable bed. To account for the non-hydrostatic pressure distribution caused by the vertical acceleration of fluid particles, these authors introduced a method very similar to one suggested by Boussinesq (1877). An empirical determination of the distance by which the sediment transport rate lags the shear stress at the bed made it possible to predict the condition for stable and unstable bed. This method made it possible to investigate even the occurrence of three-dimensional bed waves.

The theory of bed-wave formation in erodible channels seems to have reached a stage where further progress must depend on improved account of the physical mechanisms involved. The formation of lower-régime bed waves (ripples, dunes) starts at very low sediment transport rates, where the sand particles move essentially as bed load. Upper-range bed waves (standing waves, antidunes), on the other hand, occur when the sediment transport is vigorous, so it is natural to assume that sediment transport in suspension will be a significant feature of this range.

This paper presents a mathematical model of flow over a sinusoidal, movable bed. An attempt has been made to introduce some additional features in the description in order to account for the most important physical effects responsible for the bed wave formation. Even so, the model makes use of some rather drastic simplifications in order to permit a reasonably convenient mathematical description.

The theory of transport by suspension in common use was developed by Rouse (1939) and verified experimentally by Vanoni (1946). This theory deals with the distribution of sediment concentration c under strictly uniform flow conditions. In practice, however, the flow will usually be non-uniform as a result of standing waves and antidunes. Then the distribution of sediment concentration will be non-uniform, too, and in order to account for this in a reasonably simple way we proceed to replace the Rouse–Vanoni distribution with the less accurate exponential distribution (of equation (5)) mentioned by Brown (1949). This corresponds to a constant value of the eddy diffusivity ϵ_d over the whole depth, and is known to be a crude approximation close to the bed. Hence, we have to introduce a value of the sediment concentration at the bed, c_{b0}, different from the one actually occurring.

When the diffusivity is specified, the non-uniform sediment distribution may be accounted for by an equation describing the equilibrium between convection, settling and diffusion.

The two-dimensional flow of a real fluid over a sinusoidal bed is described by the vorticity transport equation, using the eddy viscosity concept.

Then, a linear stability analysis may be carried out in the conventional way, the plane bed being stable only if flow conditions are such that the amplitude of the sinusoidal bed waves is attenuated.

2. Velocity and sediment distribution in uniform channel flow

One of the basic difficulties in the formulation of a satisfactory mathematical model of erodible bed instability is that it must account for the non-hydrostatic pressure distribution as well as fluid friction. Moreover, a complete theory of non-uniform turbulent shear flow does not exist at present, and consequently some kind of a semi-empirical turbulence theory must be applied.

The eddy viscosity concept, which has been surprisingly successful in calculations of self-preserving boundary layers and uniform channel flow, will be used here as an approximation for slightly non-uniform flow.

To avoid very complicated calculations it is desirable to apply a constant value of the eddy viscosity ϵ, and this is, in fact, possible within the frame of a technical turbulence theory if an adequate boundary condition is applied, as suggested by the author (1964). To illustrate the method, it is appropriate to consider first the simple case of a uniform, steady and two-dimensional channel flow. In the case of hydraulic rough bed, the velocity profile is given by

$$\frac{U}{U_{f0}} = 8{\cdot}5 + 2{\cdot}5 \ln \frac{x_2}{k}, \tag{1}$$

in which U is the velocity, x_2 the distance from the bed, k the equivalent sand roughness, and U_{f0} the friction velocity defined by

$$U_{f0} = (\tau_0/\rho)^{\frac{1}{2}}, \tag{2}$$

where τ_0 denotes the bed shear stress and ρ the fluid density. In the major part of the flow (outside the constant stress layer) the velocity profile is alternatively well described by the parabolic velocity distribution obtained from integration of the flow equation, assuming a constant value of the eddy viscosity ϵ

$$U = U_{b0} + \frac{DU_{f0}^2}{\epsilon}\left[\frac{x_2}{D} - \frac{1}{2}\left(\frac{x_2}{D}\right)^2\right], \tag{3}$$

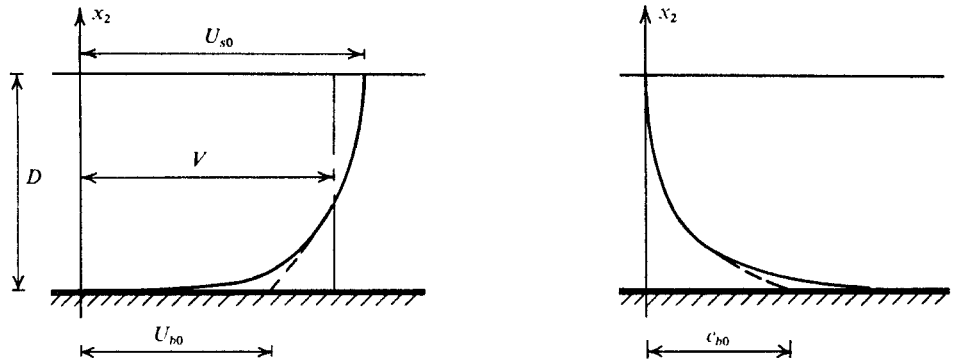

FIGURE 1. Velocity and sediment concentration distributions in uniform channel flow.

in which D is the flow depth, see figure 1. Instead of the rather abrupt logarithmic fall towards the wall, the parabolic velocity profile takes a finite U_{b0} at the bed level, subscript 0 referring to the uniform state of flow. ϵ and U_{b0} are easily evaluated by matching the two profiles at the outside of the constant stress layer. In this way it was found that

$$\epsilon = 0{\cdot}077 U_{f0} D \tag{4}$$

(cf. Hinze 1959) and that for rough walls U_{b0} is determined by the equation

$$\frac{U_{b0}}{U_{f0}} = 1{\cdot}9 + 2{\cdot}5 \ln \frac{D}{k} = K, \tag{5}$$

suggested by Engelund (1964).

The next problem is to create a reasonable model of the sediment distribution. In the case of steady, uniform flow the distribution of the volume concentration c_0 is determined by the condition of equilibrium between settling and diffusion, expressed in the equation

$$wc_0 + \epsilon_d \frac{dc_0}{dx_2} = 0,$$

where w is the fall velocity of the sediment grains (Rouse 1939). If, as suggested by Brown (1949), the diffusivity ϵ_d is replaced by the constant value of the eddy viscosity ϵ, the solution is

$$c_0 = c_{b0} \exp(-wx_2/\epsilon), \tag{6}$$

in which c_{b0} is a nominal concentration at bed level. Because the variation of ϵ has been neglected, the values of c_0 predicted from (6) are generally somewhat smaller than the actual concentrations, see figure 1.

In order to relate the bed concentration c_{b0} to the bed shear stress we must try to estimate the total rate of suspended transport

$$q_{s0} = \int_0^D U c_0 dx_2 \approx V c_{b0} \epsilon / w, \tag{7}$$

applying (6) and replacing the variable flow velocity U (cf. equation (3)) by the mean velocity V.

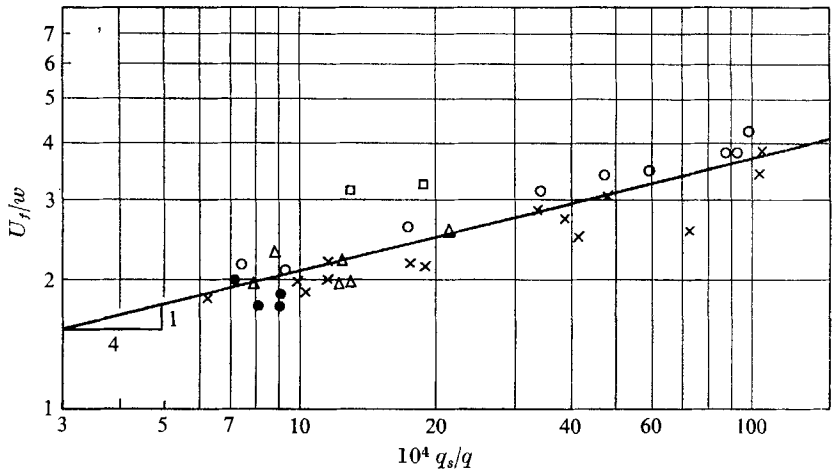

FIGURE 2. Suspended sediment transport relation. Simons, $d = 0{\cdot}19$ mm, $d = 0{\cdot}28$ mm. Brooks, $d = 0{\cdot}16$ mm, $d = 0{\cdot}10$ mm. Nomicos, $d = 0{\cdot}137$–$0{\cdot}152$ mm.

For the average concentration, obtained by dividing q_{s0} by the fluid discharge $q = VD$, the following empirical formula is suggested

$$\frac{q_{s0}}{q} = \alpha \left(\frac{U_{f0}}{w} \right)^4. \tag{8}$$

In figure 2, (8) is compared with some experiments in which the suspended load was a dominating part of the total sediment transport. The bed configuration was in all cases antidunes or plane bed. The formula is not assumed to be more accurate than most other transport formulae. It has been applied mostly because of its convenience. From (7) we now find

$$\frac{q_{s0}}{q} = \frac{\epsilon c_{b0}}{wD},$$

and after substitution of (4) and (8):

$$c_{b0} = 13 \alpha U_{f0}^3 / w^3. \tag{9}$$

This result is immediately seen to make physical sense: The square of the friction velocity equals the kinematical shear stress. The larger the shear stress, the

more violent is the tendency for fluid turbulence to pick up sediment particles from the bed. Similarly, the larger the settling velocity w, the more pronounced is the tendency for sediment particles near the bottom to leave the state of suspension by settling. Hence, it seems quite reasonable that the bottom concentration c_{b0} is determined by the ratio between the friction and the settling velocity, in accordance with (9).

The non-dimensional factor α will probably depend on the sediment properties but has been put equal to 0·00056 in the present analysis; a value appropriate for the data plotted in figure 2.

Besides the suspension, a certain part of the sediment moves as the bed load, i.e. in more or less continuous contact with the bed. The rate of bed load transport q_b has been found to follow the relation (Meyer-Peter & Müller 1948)

$$\Phi_b = \frac{q_b}{((s-1)gd^3)^{\frac{1}{2}}} = 8(\theta - 0{\cdot}047)^{\frac{3}{2}}, \tag{10}$$

in which s is the relative density of the sediment grains, g the acceleration of gravity, d the characteristic grain diameter, and θ the non-dimensional tractive force defined by

$$\theta = \frac{U_f^2}{(s-1)gd}. \tag{11}$$

The statements made so far are all concerned with the steady and uniform state of flow. For gradually varied flow some further assumptions have to be introduced. Probably, the most convenient and yet physically plausible step is to assume that the bottom concentration c_b and the bed load transport q_b respond to changes of the shear without any lag, so that c_b and q_b still vary according to (9), (10) and (11), respectively, but with the local value of U_f substituted.

3. The basic equations

Under the assumptions stated in the previous section, the flow may be described by the vorticity transport equation

$$\frac{d\omega}{dt} = \epsilon \nabla^2 \omega,$$

for two-dimensional flow, the vorticity being defined by the equation

$$2\omega = \frac{\partial v_2}{\partial x_1} - \frac{\partial v_1}{\partial x_2};$$

x_1 is a co-ordinate in the mean flow direction as indicated in figure 3; v_1 and v_2 are the velocity components.

Now it is assumed that flow consists of small, periodic perturbations superposed on a uniform flow of the type described in § 2. If the bed form is assumed to migrate with the velocity a_r in the flow direction, the boundary slip velocity given by (5) must be modified to

$$U_b = U_f K + a_r, \tag{12}$$

where U_f is the local value of the friction velocity, calculated along the bed surface from the expression

$$U_f^2 = \frac{\tau}{\rho} = \epsilon\left(\frac{\partial v_1}{\partial x_2} + \frac{\partial v_2}{\partial x_1}\right). \tag{13}$$

The stream function ψ for the perturbation is defined by

$$v_1 = U - \frac{\partial \psi}{\partial x_2} \quad \text{and} \quad v_2 = \frac{\partial \psi}{\partial x_1},$$

in which U is the unperturbed velocity, given by (3). The vorticity ω becomes

$$2\omega = -U' + \nabla^2\psi,$$

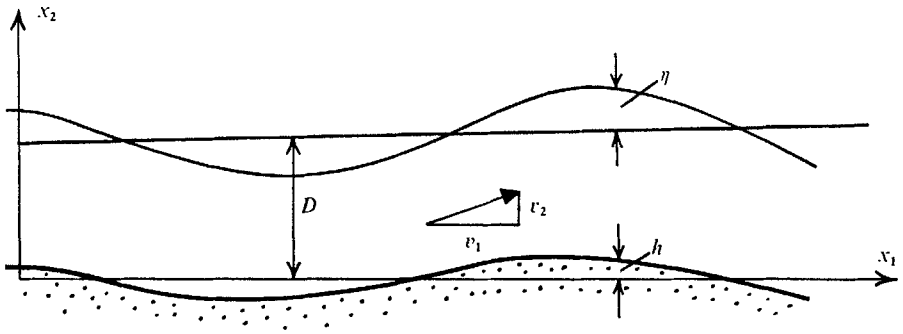

FIGURE 3. Definition sketch.

the prime indicating differentiation in the x_2-direction. If this expression is substituted into the vorticity transport equation and only first-order terms are retained, we get

$$\frac{\partial}{\partial t}(\nabla^2\psi) + U\frac{\partial}{\partial x_1}(\nabla^2\psi) - U''\frac{\partial \psi}{\partial x_1} = \epsilon\nabla^4\psi. \tag{14}$$

Next we consider the distribution of the suspended sediment load in a non-uniform flow. It is described by a local continuity equation expressing the equilibrium between settling, diffusion and convection.

The sediment flux due to settling is equal to $c\mathbf{w}$, where $\mathbf{w}$ is the sediment fall velocity vector. If ϵ is the diffusivity, the sediment flux caused by diffusion equals $\epsilon \operatorname{grad} c$.

Hence, for a unit volume of the water sediment mixture, we obtain the following equation of continuity

$$\frac{dc}{dt} = \operatorname{div}(-c\mathbf{w} + \epsilon \operatorname{grad} c),$$

or

$$\frac{dc}{dt} = w\frac{\partial c}{\partial x_2} + \epsilon\nabla^2 c.$$

When the uniform flow is perturbed, the concentration c is given by

$$c = c_0 + \tilde{c},$$

in which the perturbation $\tilde{c}$ is supposed to be small compared with the value c_0 pertaining to the uniform state. Hence, within the frame of a first-order theory, the local continuity equation becomes

$$\frac{dc}{dt} = \frac{d\tilde{c}}{\partial t} + U\frac{\partial \tilde{c}}{dx_1} + \frac{\partial \psi}{\partial x_1}\frac{dc_0}{dx_2} = w\frac{\partial \tilde{c}}{\partial x_2} + \epsilon\nabla^2\tilde{c}. \tag{15}$$

Now it is convenient to introduce dimensionless space and time variables, putting

$$\xi_i = x_i/D, \quad t' = Vt/D,$$

and to express the periodicity of the flow perturbations by

$$\left.\begin{aligned} \psi/VD &= f(\xi_2)\exp\left[\iota kD\left(\xi_1 - \frac{a}{V}t'\right)\right], \\ \tilde{c} &= \phi(\xi_2)\exp\left[\iota kD\left(\xi_1 - \frac{a}{V}t'\right)\right], \end{aligned}\right\} \tag{16}$$

in which f and ϕ are unknown functions, ι the imaginary unit and k the wave-number. Further

$$a = a_r + \iota a_i$$

is a complex migration velocity of the bed waves. The real part equals the velocity introduced in (12). When the expressions (16) are substituted into (14) and (15), we obtain the following pair of ordinary differential equations in f and ϕ:

$$(U-a)[f'' - (kD)^2 f] - U''f = \frac{\epsilon}{\iota kD^2}[f^{\mathrm{iv}} - 2(kD)^2 f'' + (kD)^4 f], \tag{17}$$

$$\phi'' - (kD)^2\phi + \frac{wD}{\epsilon}\phi' - \frac{\iota kD^2}{\epsilon}(U-a)\phi = \left(\iota kD\frac{VD}{\epsilon}\frac{dc_0}{dx_2}\right)f. \tag{18}$$

The perturbation of the sand bed is described by the local height h of the bed above the x_1 axis, see figure 3, and is supposed to vary according to the expression

$$h = h_0\exp\left[\iota kD\left(\xi_1 - \frac{a}{V}t'\right)\right]. \tag{19}$$

Similarly, the water surface deviates from the unperturbed level by

$$\eta = \eta_0\exp\left[\iota kD\left(\xi_1 - \frac{a}{V}t'\right)\right]. \tag{20}$$

For convenience the bed-wave amplitude h_0 is considered real. Only if the water surface amplitude η_0 turns out to be real also, will the surface undulation be in phase with the bed wave.

The final relationship of interest is the continuity of the total sediment movement. The total transport rate q_t is now written as the sum of the bed load and the suspended loads

$$q_t = q_b + \int_h^{D+\eta} v_1 c\, dx_2. \tag{21}$$

For an unsteady situation we get the following relation

$$\partial q_t/\partial x_1 = -(1-n)\partial h/\partial t, \tag{22}$$

in which n is the porosity of the sand bed.

4. The boundary conditions

(i) First we consider the kinematical boundary condition for the sand bed, expressed as

$$\frac{dh}{dt} = \frac{\partial h}{\partial t} + U_b \frac{\partial h}{\partial x_1} = v_2,$$

where v_2 is the vertical component at bed level to be calculated from the stream function ψ. When (16) is introduced, the boundary condition is reduced to

$$Vf(0) = \frac{h_0}{D}(U_{b0} - a). \tag{23}$$

(ii) Secondly, we consider the shear stress along the bed, as obtained from (13). The boundary condition is given by (12), so that

$$\tau/\rho = (U_b - a_r)^2/K^2.$$

By the introduction of the stream function, the left-hand side becomes

$$\frac{\tau}{\rho} = U_{f0}^2\left(1-\frac{h}{D}\right) - \frac{\epsilon V}{D}[f''(0) + (kD)^2 f(0)]\exp\left[\iota kD\left(\xi_1 - \frac{a}{V}t'\right)\right].$$

For the quantity $U_b - a_r$ on the right-hand side we get similarly

$$U_b - a_r = U_{b0} - a_r + U'h - Vf'(0)\exp\left[\iota kD\left(\xi_1 - \frac{a}{V}t'\right)\right].$$

When these expressions and (23) are combined, we get the first-order approximation

$$f''(0) + c_1 f'(0) + c_2 f(0) = 0, \tag{24}$$

where the coefficients are given by the following expressions

$$c_1 = -\frac{26}{K} \quad \text{and} \quad c_2 \simeq (kD)^2 + \frac{13}{K} + 2\left(\frac{13}{K}\right)^2.$$

(iii) The third condition at the bed is based on the relation between the bed concentration c_b and the local value of the shear stress. As accounted for in § 2, it is assumed that c_b varies according to (9), so that along the bed surface

$$c_b = 13\alpha U_f^3/w^3 = \frac{13\alpha}{w^3}\left(\frac{\tau}{\rho}\right)^{\frac{3}{2}}.$$

In formulating the previous boundary condition we derived an expression for τ. The analogous expression for c_b is

$$c_b = c_{b0} + c_0' h + \phi(0)\exp\left[\iota kD\left(\xi_1 - \frac{a}{V}t'\right)\right].$$

After substitution and linearization this boundary condition appears:

$$f'(0)+\frac{U_{b0}-a_r}{3Vc_{b0}}\phi(0)=\frac{h_0}{D}\left(\frac{13U_{f0}}{V}+\frac{wD(U_{b0}-a_r)}{3V\epsilon}\right). \tag{25}$$

(iv) The kinematical boundary condition for the water surface is exactly analogous to the condition for the bed and turns out to be

$$Vf(1)=\frac{\eta_0}{D}(U_{s0}-a). \tag{26}$$

That the normal stress vanishes at the free surface is, to the first-order approximation, expressed as

$$\frac{p_s}{\rho}-2\epsilon\frac{\partial v_2}{\partial x_2}=0,$$

when the surface tension is neglected and p_s is the water pressure just below the surface. From this, we get

$$\frac{p_s}{\rho}=\frac{2\epsilon V}{D}\,\iota kDf'(1)\exp\left[\iota kD\left(\xi_1-\frac{a}{V}t'\right)\right].$$

Next, the equation of motion for $\xi_2=1$ becomes

$$\frac{dv_1}{dt}=-\frac{\partial}{\partial x_1}\left[g\eta+\frac{p_s}{\rho}\right]+\epsilon\nabla^2 v_1+gS,$$

in which S is the mean slope of the channel. In this the velocity v_1 is expressed in terms of the stream function and the following relation pertaining to the uniform flow is applied:

$$\epsilon U''+gS=0,$$

where S is the slope. Then the boundary condition becomes

$$f''(1)+\left[-3(kD)^2-\frac{\iota kD}{U_{f0}}13(U_{s0}-a)\right]f'(1)+13\,\frac{\iota kDV^2}{U_{f0}F^2(U_{s0}-a)}f(1)=0. \tag{27}$$

(v) The shear stress must vanish at the free surface, which gives the condition

$$U_{f0}^2\frac{\eta_0}{D}=\frac{\epsilon V}{D}[f''(1)+(kD)^2f(1)],$$

or by the substitution of (26)

$$f''(1)+f(1)\left[(kD)^2+\frac{13}{K}\right]=0. \tag{28}$$

(vi) The last boundary condition is that the vertical sediment flux

$$\epsilon\frac{\partial\tilde{c}}{\partial x_2}+w\tilde{c}$$

vanishes at the water surface. This gives the condition

$$-\phi'(1)=\frac{wD}{\epsilon}\phi(1). \tag{29}$$

This ends the formulation of the boundary conditions.

5. The case of negligible bed load

As the basic equations and boundary conditions have been developed, we are now able to carry out a stability analysis, that is, to predict under what conditions the initial bed wave amplitude h_0 will decrease or increase. As an important special case we consider first the instability corresponding to flow conditions such that the bed load may be neglected. This situation will occur for fine sediments and the rather high flow rates associated with large Froude numbers. Hence, the assumption of negligible bed load may be assumed to yield a fair description of the so-called upper-range bed configuration corresponding to supercritical flow.

The total rate of suspended sediment transport is then found from

$$q_s = \int_h^{D+\eta} v_1 c \, dx_2$$

$$\simeq VD \int_{h/D}^1 \left\{ U/V - f' \exp\left[\iota kD \left(\xi_1 - \frac{a}{V} t' \right) \right] \right\} \left\{ c_0 + \phi \exp\left[ikD \left(\xi_1 - \frac{a}{V} t' \right) \right] \right\} d\xi_2.$$

Introducing the sediment transport q_{s0} for uniform flow, this equation may be written in the form

$$\frac{q_s - q_{s0}}{VD} = -c_{b0} \frac{h}{D} \frac{U_{b0}}{V} + \int_0^1 [U\phi(\xi_2)/V - c_0 f'(\xi_2)] \exp\left[\iota kD \left(\xi_1 - \frac{a}{V} t' \right) \right] d\xi_2.$$

Substituting this and (19) into the continuity equation (22) for the sediment, we get

$$\frac{(1-n)a}{V} = -c_{b0} \frac{U_{b0}}{V} + \frac{D}{h_0} \int_0^1 (U\phi/V - c_0 f') \, d\xi_2. \tag{30}$$

The first step in the stability analysis is of course the solution of the basic equations (17) and (18), cf. Engelund (1968).

Actually, (17) is of the Orr–Sommerfeld type but is easy to solve because no critical layer is present. In the first approximation the bed migration may be neglected putting $a = 0$. The complete solution comprises four independent particular solutions. When the function f has been found, the complete solution of (18) is the sum of a particular solution and the complete solution of the homogeneous equation.

Then from (30) a preliminary value of the migration velocity a is obtained. By a straightforward and rapidly converging iteration procedure, the functions f and ϕ are corrected, and the final value of a is determined. This quantity, in general complex, depends on the following non-dimensional parameters

$$F = V/(gD)^{\frac{1}{2}}, kD, U_{f0}/w \quad \text{and} \quad K \,(\text{or } V/U_{f0}).$$

In figure 4 the imaginary part a_i of the migration velocity is plotted against the Froude number F for reasonable, though arbitrary values of the parameters.

For the example denoted by the dotted line, a_i is negative for all Froude numbers, indicating stability of the flow.

The example denoted by the full line, however, is typical of the unstable situation. There is a zero of a_i for a Froude number near the critical ($F_1 \sim 1{\cdot}1$) and another zero for a larger Froude number ($F_2 \sim 1{\cdot}6$).

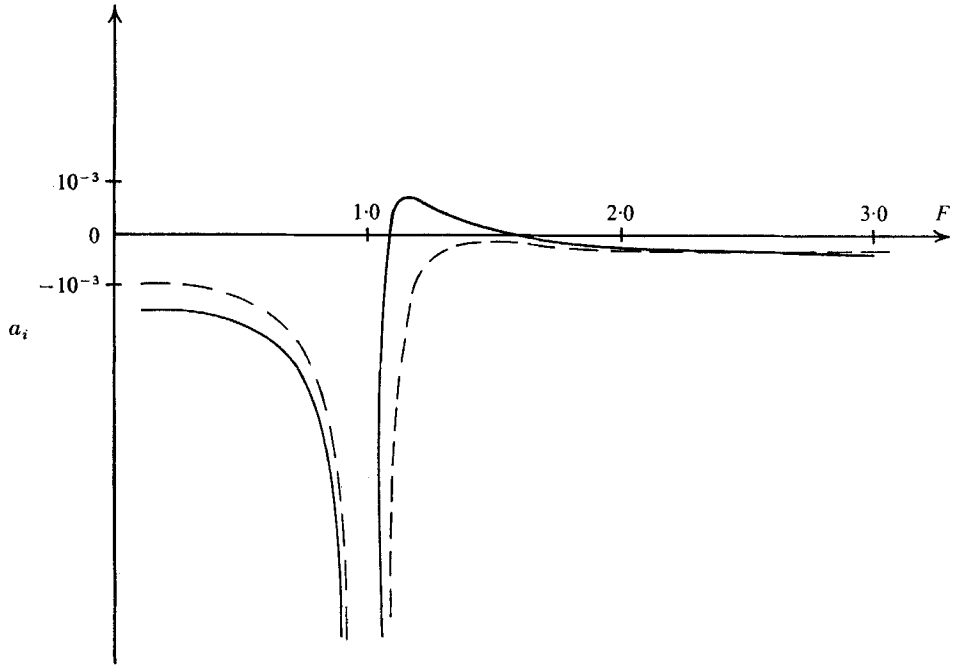

FIGURE 4. Variation of the imaginary part of the bed wave celerity as a function of the Froude number F. The examples correspond to the parameter values $U_f/w = 1$ and $V/U_f = 17$. The full line indicates $kD = 0{\cdot}4$, the dashed line $kD = 0{\cdot}25$.

The zeros indicate points of neutral stability, and for Froude numbers in the interval $F_1 < F < F_2$ we find positive values of a_i, corresponding to instability.

When a sufficient number of such calculations has been carried out, we are able to work out a stability diagram like that presented in figure 5. The curves of neutral stability form a parametric family of loops, the parameter being U_f/w. The diagram corresponds to a constant value of the second parameter V/U_f, but is not sensitive to changes in that value.

The unstable area is bounded by two dashed, limiting curves, actually well known from previous investigations. The upper limiting curve is the stability boundary predicted from potential theory by Reynolds (1965), given by the equation

$$F^2 = \coth(kD)/kD.$$

The lower limiting curve corresponds to the condition of critical flow

$$F^2 = \tanh(kD)/kD.$$

That this curve is a stability boundary seems to be a new interpretation, as according to potential analysis this curve marks the transition from antidunes to dunes. Under these circumstances it may be of interest to consult some suitable experimental evidence, such as the flume data reported by Kennedy (1961) and by

Guy, Simons & Richardson (1966). These data plotted in figure 6 correspond to the flow configuration characterized as standing waves or antidunes. If cases of a predominant three-dimensional character of the flow were disregarded, the agreement between theory and experiments would be still more convincing.

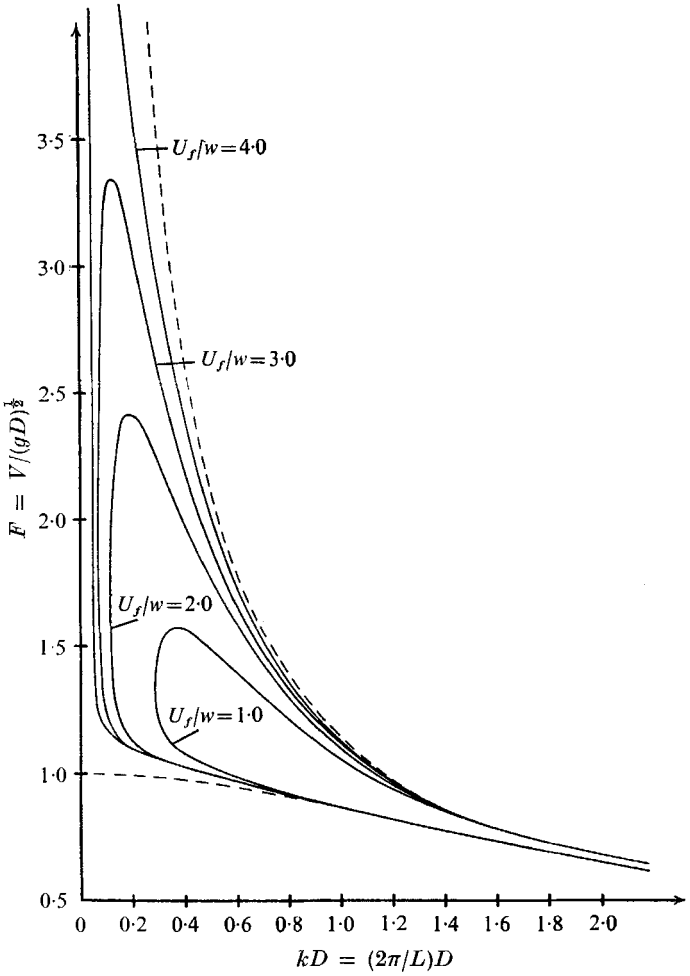

FIGURE 5. Stability diagram for the case of negligible bed load, corresponding to $V/U_f = 17$.

It should be pointed out that the assumption of negligible bed load restricts the validity of the result to experiments with rather fine sediment. For the case of rather coarse sediment we can no longer be sure that there is a stable region for subcritical flow conditions. The problem will be further elucidated in § 7.

6. Discussion of results

The agreement between the theoretical stability analysis and the observations does not necessarily imply that the model is in accordance with the actual mechanism of instability. Hence, it is of interest to describe the details of some

specific examples and to compare the flow patterns and the sediment distribution with general experience from flume investigations.

As the first example consider a flow situation corresponding to a point situated at the lower branch of a curve of neutral stability, see figure 7. It is typical that the antidune is moving rapidly upstream and that the bed wave amplitude is

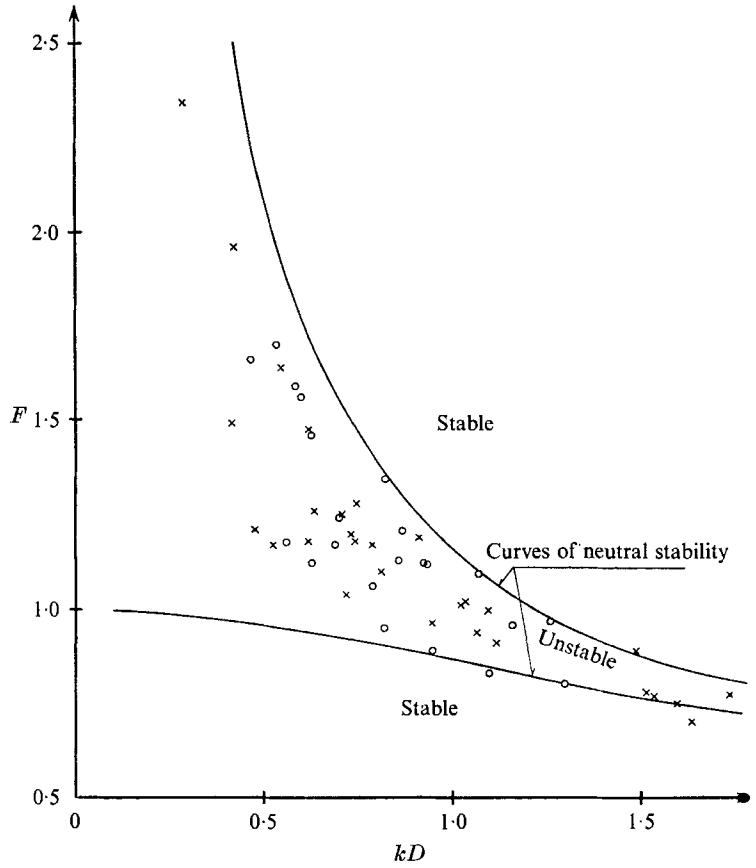

FIGURE 6. Asymptotic stability boundaries. Experiments by Guy, Simons & Richardson (1966): ○, d = 0·19–0·47 mm; and by Kennedy (1961): ×, d = 0·23–0·55 mm.

only about 5 % of the surface wave amplitude, so that the bed will appear nearly plane. There is a rather large phase shift (about 32°) between surface waves and bed waves, as is often observed in the laboratory, for example, by Kennedy (1961).

The bed concentration is largest near the troughs, where the largest flow velocity occurs, and smallest near the crest of the surface wave, while the concentration at higher levels exceeds what corresponds to the undisturbed concentration distribution. Considering the flow from trough to crest, we realize that along this stretch the suspended sediment is gradually elevated. A corresponding lowering of the suspended material is realized along the stretch from

crest towards trough. This characteristic non-uniform distribution of the sediment is well known from experiments.

Figure 8 illustrates the flow corresponding to a point of the upper branch of the same curve of neutral stability. Under these circumstances the flow situation is strikingly different from the one considered above. The bed waves are now moving

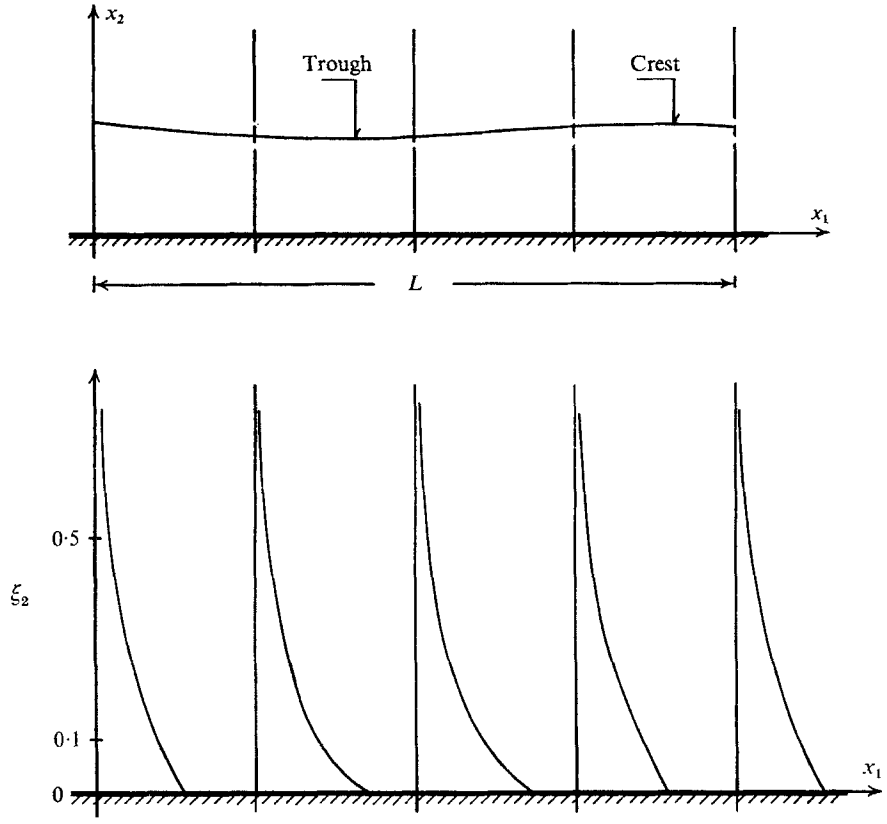

FIGURE 7. Flow pattern and concentration distributions for a neutrally stable bed wave for the lower branch of a stability curve. The example corresponds to the parameters $U_f/w = 3$, $kD = 1$ and $F = 0{\cdot}866$.

very slowly and their amplitude is only slightly smaller than that of the surface waves. The phase shift is small and the concentration distribution is not very different from one vertical to another.

Finally, we consider an unstable situation corresponding to a Froude number between the two considered before, see figure 9. The general description of the flow is not very different from that pertaining to figure 7, the most crucial difference being that the vertical gradient of the concentration is much smaller above the crest than above the trough. This means that sedimentation takes place at the crest and erosion occurs at the trough, thus increasing the bed wave amplitude corresponding to instability.

Another interesting result of the present analysis is that it introduces effects not accounted for by potential theory.

First, we note that curves of neutral stability now do not extend to infinity, which explains how a plane stable bed may occur for large Froude numbers, as reported by Kennedy (1961).

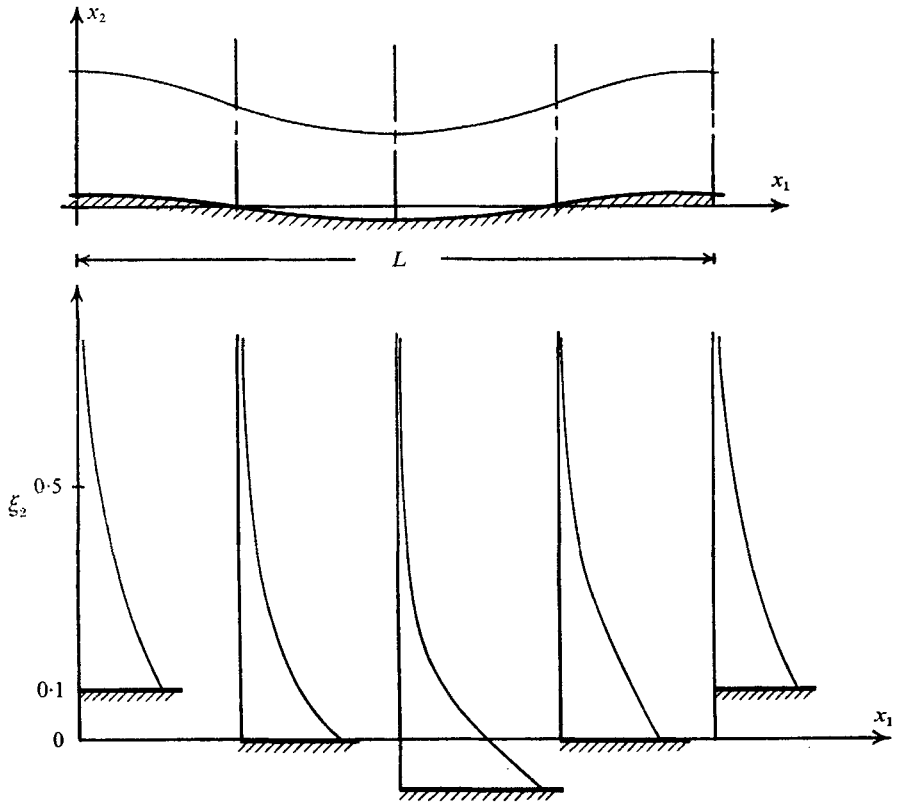

FIGURE 8. Flow pattern and concentration distributions for a neutrally stable bed wave for the upper branch of a stability curve. The example corresponds to the parameters $U_f/w = 3, kD = 1$ and $F = 1{\cdot}128$.

Secondly, it has often been reported that periods of plane bed configuration alternate with periods of developing wave trains (antidunes). Inspection of the stability diagram reveals a possibility of heuristic explanation of this phenomenon.

Let us suppose that the average flow conditions correspond to a point situated at a curve of neutral stability. Then small fluctuations in the flow or sediment properties can cause fluctuations in the hydraulic parameters sufficient to shift from stable to unstable conditions, particularly in the regions where the location of the stability curve is very sensitive to changes in the parameter U_f/w.

7. Solution including bed load

The distinction between suspended load and bed load as well as the precise definitions of these terms have caused much trouble for several decades and a really satisfactory result has not been achieved so far. For the present model, the only important thing is that a certain amount of the total load is assumed to

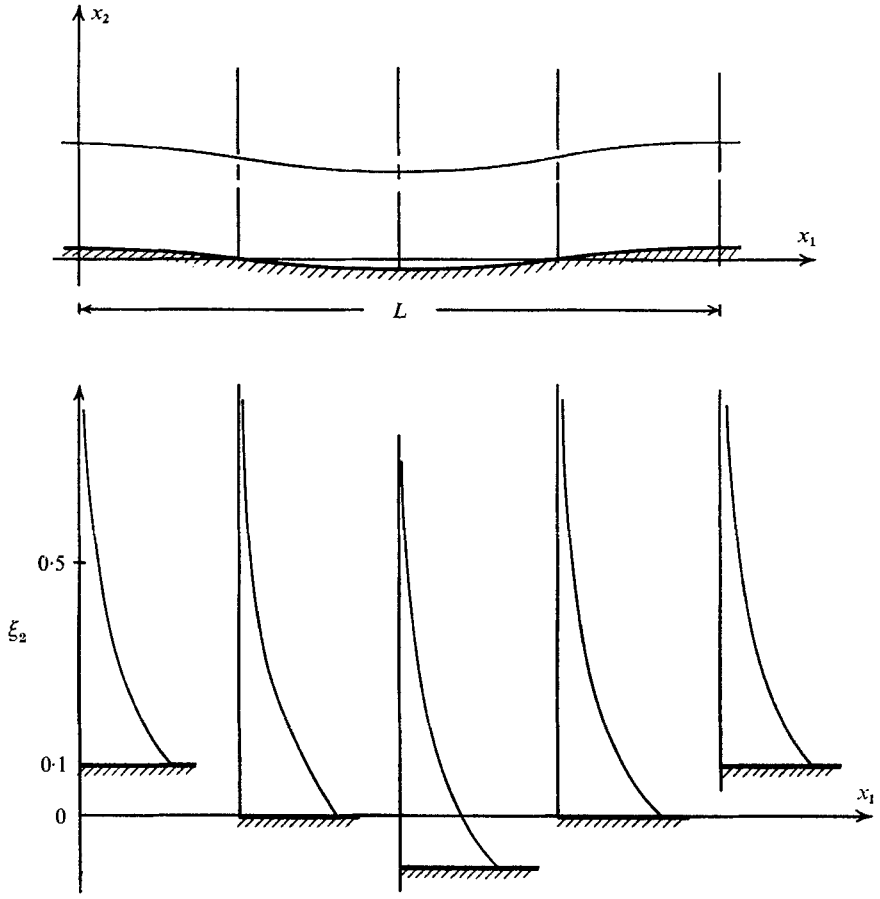

FIGURE 9. Flow pattern and concentration distribution for an unstable flow. The example corresponds to the parameters $U_f/w = 3$, $kD = 1$ and $F = 1$.

respond very quickly to changes in the tractive stress so that the spatial lag may be neglected. This part of the total load is for the present purpose assumed to be equal to the bed load as determined from (10). In effect, there is no profound theoretical or experimental support for the idea that the total sediment load is the sum of a bed load (determined from coarse material tests) and a suspended load determined from quite different flow conditions. However, for lack of better knowledge, this rather widely accepted assumption has been used in the

following in order to develop a model more plausible at small Froude numbers, where the bed load transport is usually rather dominant in practice.

The analysis described above is changed only in so far as the continuity equation (30) is concerned. Using the assumption (21), the analysis proceeds along the same lines as before.

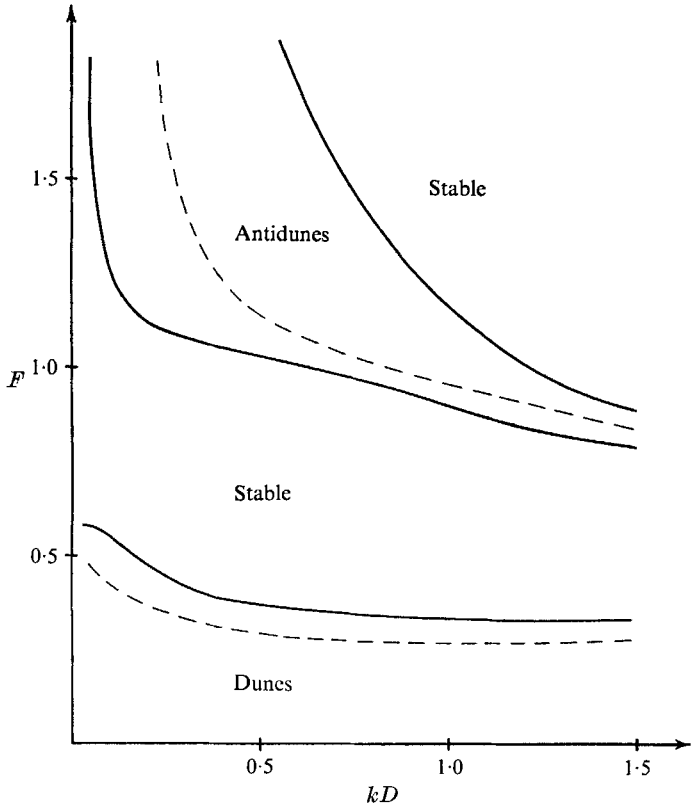

FIGURE 10. Stability diagram for the complete solution. The parameters are $V/U_f = 21$ and $U_f/(wF) = 1$.

The results of the stability analysis are most conveniently presented in a somewhat different way, corresponding to a fixed value of grain diameter d and depth D. This implies a constant value of the ratio V/U_f, at least to first approximation. Further, the friction velocity U_f must vary in direct proportion to the Froude number, as appears from the following manipulations:

$$U_f = (U_f/V)\,F(gD)^{\frac{1}{2}}.$$

For this reason the parameter $U_f/(wF)$ has been used. The second parameter is V/U_f.

From the theory of flow resistance in two-dimensional channel flow, it is known that this second parameter is related to the relative roughness of the bed by the following equation

$$\frac{V}{U_f} = 6{\cdot}0 + 2{\cdot}5 \ln \frac{D}{k}.$$

For a fixed bed, the equivalent roughness k is usually identified with the grain size d, referring to Nikuradse's test series. When sediment transport is involved, the relation is more complex, but for a plane bed or small sinusoidal undulations, it has been found that k is greater than d, probably by a factor of 2 or 3 (Engelund & Hansen 1966).

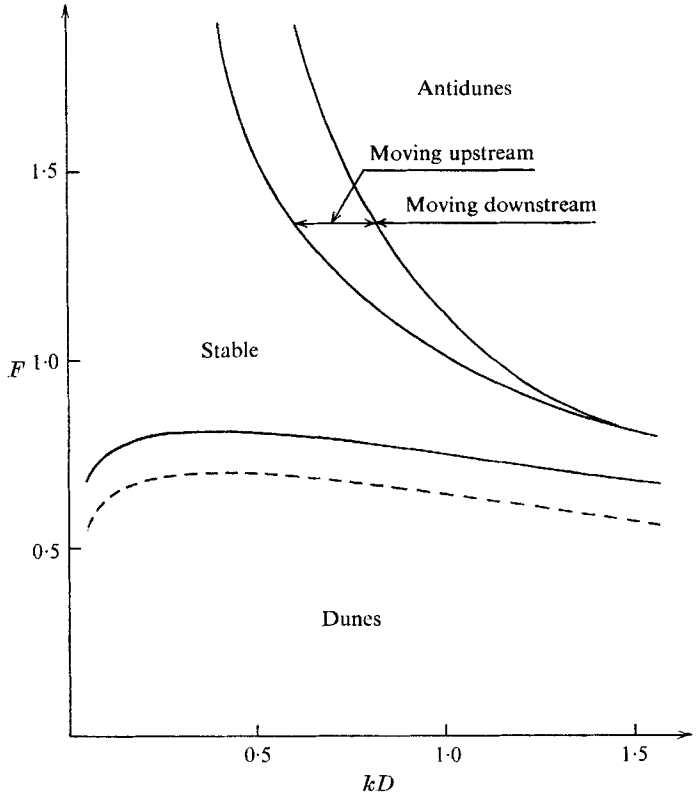

FIGURE 11. Stability diagram for the complete solution. The parameters are $V/U_f = 21$ and $U_f/(wF) = 1$.

It would require very many diagrams to cover completely the variations of the two parameters mentioned. The two typical examples given in figures 10 and 11 illustrate some features of principal interest.

The diagram presented in figure 10 is for

$$U_f/wF = 2,$$

corresponding to a rather fine sediment. The new and interesting feature is that the introduction of a bed load term creates a region of instability for small Froude numbers, while the upper stability boundary is unchanged. The perturbations are migrating downstream indicating the formation of dunes.

For a given value of kD there exists one Froude number for which the imaginary part a_i of the migration velocity is a maximum, indicating the largest growth rate of the perturbation. These values are marked by the dashed curves. As pointed

out by Kennedy (1963), these privileged undulations are of particular interest, because they may be expected to determine the wavelength actually occurring.

In figure 11 the parameter is changed to

$$U_f/wF = 1,$$

which corresponds for the same depth to a considerably larger grain size. The diagram indicates that for the coarser material the stability boundaries shift to larger values of the Froude number, which is in agreement with experimental evidence. The flow becomes stable for F greater than 3·3.

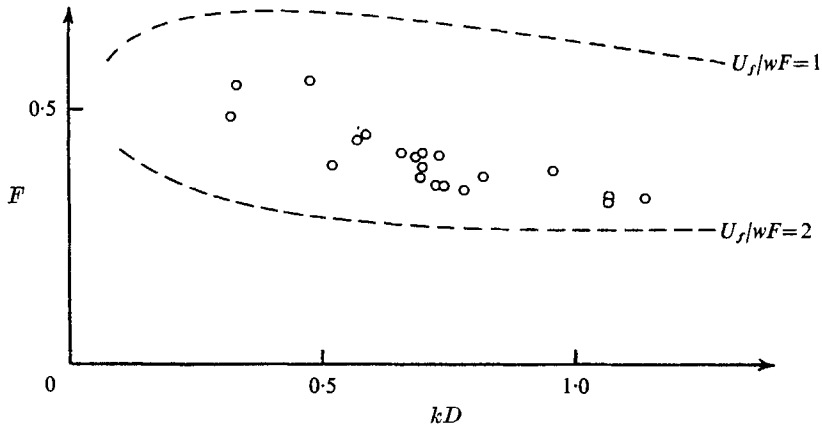

FIGURE 12. kD for dunes plotted against Froude number. Data from Guy, Simons & Richardson (1966), grain diameter d = 0·27 and 0·28 mm. The dashed curves are taken from figures 10 and 11.

Hence, in this example the upper stability boundary is changed considerably. However, the conditions in this example are very extreme, because the bed load transport is rather dominant even for high Froude numbers. Little is known about sediment transport rates under such conditions, and the change of the upper stability boundary may be due to a shortcoming of the basic sediment transport relation.

A direct comparison of theory and experiment is difficult for several reasons. One basic trouble is that the stability analysis assumes a plane bed, while the bed resulting from instability is covered by dunes, introducing considerable change of the flow resistance. Irrespective of this, actually measured values of the Froude number, when plotted against kD, exhibit a general trend (figure 12) similar to the theoretical predictions indicated in the previous figures. The data (Guy *et al.* 1966) correspond to the grain size $d = 0{\cdot}27 - 0{\cdot}28$ mm.

8. Possibility of improving the model

In some respects the model presented may be characterized as a rather crude one. For this reason the author should like to comment on the possibility for improvement.

The most obvious possibility is to take into account the variation of the diffusivity. This would give a more satisfactory description of the velocity and sediment distributions near the bed.

This, however, is unlikely to yield any fundamental changes in the results or to add essentially new features to the description.

The author is indebted to Ove Skovgaard, for able assistance and programming. Dr Carl F. Nordin and Dr Eggert Hansen commented on the first draft and suggested improvements. Further, the author is indebted to Dr A. J. Reynolds, Brunel University, for stimulating discussions of the subject.

REFERENCES

ALLEN, J. R. 1968 *Current Ripples.* Amsterdam: North-Holland.

BOUSSINESQ, J. 1877 Essai sur la theorie des eaux courantes. *Sci Math. et Phys.* Tome XXIII.

BROWN, C. B. 1949 Sediment transportation. Chapter XII in *Engineering Hydraulics.* (Ed. H. Rouse) London: Wiley.

ENGELUND, F. 1964 A practical approach to self-preserving turbulent flows. *Acta Polytechnica Scandinavica,* p. 6.

ENGULEND, F. 1968 Linear theory of flow on a sinusoidal bed. *Basic Research Progress Report,* no. 17. *Techn. Univ. of Denmark,* 1–5.

ENGULEND, F. & HANSEN, E. 1966 Investigations of flow in alluvial streams. *Acta Polytechnica Scandinavica.*

GUY, H. P., SIMONS, D. B. & RICHARDSON, E. V. 1966 Summary of alluvial channel data from flume experiments. 1956–61. *Geological Survey Professional Paper* 462–I, 1–96.

HINZE, I. O. 1959 *Turbulence.* London: McGraw-Hill.

KENNEDY, J. F. 1961 Stationary waves and antidunes in alluvial channels. Rep. no. KH-R-2, *W. M. Keck Lab. of Hydraulics and Water Res., California Institute of Technology.*

KENNEDY, J. F. 1963 The mechanics of dunes and antidunes in erodible bed channels. *J. Fluid Mech.* **16**, 521–44.

MEYER-PETER, E. & MÜLLER, R. 1948 Formulas for bed-load transport. *IAHSR, Report on the Second Meeting,* vol. 3, 39–64.

REYNOLDS, A. J. 1965 Waves on the erodible bed of an open channel. *J. Fluid Mech.* **22**, 113–133.

ROUSE, H. 1939 Experiments on the mechanics of sediment suspension. *Proc. 5th Intern. Congr. Appl. Mech.*

VANONI, V. 1946 Transportation of suspended sediment in water. *Trans. ASCE,* **111**, 67–102.